Role of Crystallinity in Retention of Polymer Particle Morphology in the Presence of Compressed Carbon Dioxide

C. S. Connon,* R. F. Falk, and T. W. Randolph

Department of Chemical Engineering, University of Colorado, Boulder, Boulder, Colorado 80309

Received August 18, 1998; Revised Manuscript Received December 15, 1998

ABSTRACT: The effects of compressed carbon dioxide absorption into poly(L-lactide), poly(DL-lactide), poly(glycolide), and their copolymers were observed using EPR and mechanical creep experiments to determine the correlation between the glass transition pressure and material failure pressure. Results show polymers can retain particle morphology above the carbon dioxide suppressed glass transition pressure because of a moderate crystalline volume fraction that reduces creep rates enough to limit particle agglomeration during precipitation with a compressed antisolvent.

Introduction

Encapsulation of pharmaceutical drugs into biodegradable polymers using precipitation with a compressed antisolvent (PCA) is attractive because of high encapsulation efficiency,[1] low residual solvent levels,[2] low processing temperatures, and the production of micron-sized particles.[3,4] However, the high solubility of supercritical carbon dioxide (CO_2), which enables the rapid extraction of solvent from the polymer, also causes large quantities of CO_2 to diffuse into the polymer. Acting as a diluent, CO_2 lowers the glass transition temperature (T_g) of the polymer. Polymers susceptible to a suppression of T_g below the operating temperature of the PCA system may form agglomerated particles or thin films during precipitation. As the versatility of this processing technique grows, it is becoming necessary to understand which polymer properties help maintain desired particle morphology in the presence of supercritical CO_2.

The study of CO_2 effects on polymers is not new. T_g suppression was originally observed in the creep rates recorded for poly(carbonate) pipes pressurized with CO_2.[5] Eventually this behavior led to new production methods for polymer foams, the extraction of low molecular weight compounds from polymers, and the impregnation of polymers with chemical additives.[6] Experimental measurements of T_g suppression by CO_2 include observing the relaxation of mechanical properties,[7] differential scanning calorimetery,[8] and creep compliance.[9] Thermodynamic models using lattice fluid theory and the Gibbs−Di Marzio criterion predict glass transition temperatures as a function of pressure remarkably well.[10,11] Together, models and experiments led to the classification of four fundamental polymer behaviors, and the understanding that the T_g of a polymer or copolymer at a particular pressure depends on the pure polymer T_g and the solubility of CO_2 within the polymer.

Bodmeier et al.[12] reported some interesting observations while determining suitable polymers for PCA. Bodmeier et al.[12] based the compatibility of a polymer on the degree of swelling observed in compressed CO_2. From the six polymers investigated, they reported the highly crystalline and the semicrystalline polymers were generally unaffected by high-pressure CO_2 exposure, while all the amorphous polymers agglomerated under similar conditions. This raises an interesting question of whether, in addition to polymer−CO_2 interaction characteristics, the polymer crystallinity assists in maintaining particle morphology in the presence of compressed CO_2. This paper explores the role polymer crystallinity plays in maintaining PCA particle morphology.

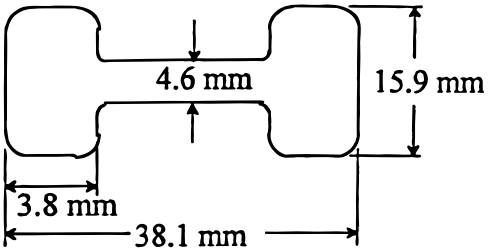

Figure 1. Standard tensile specimen.

Methodology

The following chemicals were used as received: poly(DL-lactide-*co*-glycolide) (50:50, 65:35, 75:25, 85:15) and poly(glycolide) (T_g = 35−40 °C) from Sigma; poly(L-lactide) Resomer L206 and poly(DL-lactide) Resomer R206 (T_g = 55−60 °C) from Boehringer Ingelheim; poly(DL-lactide-*co*-glycolide) (85:15) from Purac America; methylene chloride (CH_2Cl_2) from Fisher; and the molecular probe 16-doxyl-stearic acid from Aldrich.

To provide accuracy between pressure measurements made on two separate systems, the pressure transducers were calibrated from 0 to 60 MPa using a Heise gauge with accuracy to ±0.01 MPa.

Creep Experiments. Standard tensile specimens (Figure 1) were fashioned in a stainless steel mold enclosed by glass slides by heating the polymer to temperatures slightly above their melt temperature. When the polymer filled the mold, the specimen was cooled slowly by turning off the heat source. After removal from the mold, polymer specimens were suspended by one end inside an optically accessible pressure chamber. Suspension from the thick portion ensured failure occurred away from locations of point loading.

The chamber was initially charged with carbon dioxide to a pressure of 4 MPa and a temperature of 35 °C. The pressure was controlled using an ISCO compressed gas pump in the constant pressure mode and measured using a digital pressure transducer (Omega). Chamber temperatures were maintained using an air bath surrounding the test chamber. An Omega

10.1021/ma9813035 CCC: $18.00
Published on Web 02/25/1999

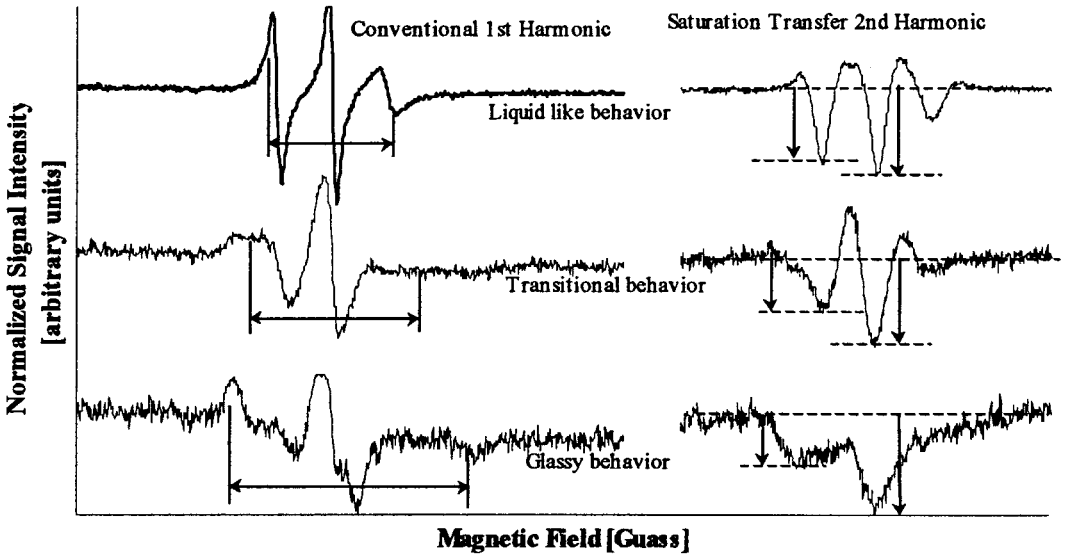

Figure 2. Presentation of both conventional first harmonic and saturation transfer second harmonic EPR spectra collected for 16-doxyl-stearic acid trapped in 65:36 poly(DL-lactide-*co*-glycolide) in the presence of CO_2 at 35 °C. EPR cell pressure starting from the top and working down: 5.5 MPa, 3 MPa, and atmospheric conditions.

thermocouple and temperature control unit controlled air temperature.

The system equilibrated for 1 h at the initial pressure and temperature setting, upon which the pressure was raised 0.5 MPa every hour thereafter. Changes in surface color/texture and gauge length were monitored. The test concluded when the specimen broke or elongated substantially within 1 h. Generally, no elongation occurred at any pressure other than the failure pressure. One hour increments were assumed to provide sufficient time for the CO_2 to equilibrate within the 1 mm thick sample because 1 h is the same order suggested by Berens and Huvard[13] for CO_2 equilibration within a similarly sized poly(methyl methacrylate) sample at 25 °C and 6.7 MPa.

EPR Spectrometry. Electron paramagnetic resonance (EPR) experiments were performed on a Bruker ESP300 EPR spectrometer. A high-pressure EPR cell was constructed out of a thick-walled, closed end quartz tube with the open end affixed to 6.35 mm stainless steel tube for connection to the pressurizing system. Pressure in the cell was controlled with a hand-operated syringe pump (High-Pressure Equipment) and measured with a digital pressure transducer (Omega). The carbon dioxide that feed the syringe pump passed through a scrubber to remove traces of oxygen (Labclear). Temperatures in the cell were measured with a thermocouple, and the cell was thermostated to ±0.1 °C using a liquid nitrogen boil-off and an Eurotherm temperature controller.

A 6 wt % solution of polymer in CH_2Cl_2 with approximately 100 μM concentration of the stable free radical spin probe 16-doxyl-stearic acid was injected into the EPR high-pressure cell. (Pressure tests on 16-doxyl-stearic acid up to 8 MPa showed no signs of extraction by supercritical carbon dioxide.) At this molarity the probe molecule will not affect the polymer properties and experiences negligible spin exchange. The CH_2Cl_2 was evaporated in a warm air bath, resulting in the deposit of a thin film of polymer and probe on the inside surface of the EPR high-pressure cell. To ensure removal of any residual CH_2Cl_2 from the polymer deposit, the EPR cell was placed under vacuum. Results could be collected from a single cell more than once to observe any shift in pressure of the transitional behavior that may have resulted from residual CH_2Cl_2. Methylene chloride is extremely soluble in CO_2 and will be completely removed from the polymer film after a single pressurized run. Using a CH_2Cl_2 solution ensures that the deposited polymer physically entraps the probe molecule; as a result, local polymer properties govern the probe molecule's behavior.

Measurements were made using two different methods: a conventional first harmonic spectrum extrema separation technique and a saturation transfer phase sensitive detection scheme sensitive to slow motion which maps the peak ratio of the second harmonic spectra. For the first technique, conventional, a first harmonic X-band EPR spectrum was recorded using a modulation amplitude of 1 G, a 100 kHz modulation frequency, a time constant of 20.48 ms, and a microwave power of 10 mW. Each recorded spectrum was the average of three 84 s, 200 G scans. In the second technique, saturation transfer, the out-of-phase second harmonic of X-band EPR spectrum was recorded using a modulation amplitude of 10 G, a 50 kHz modulation frequency, a time constant of 5.12 ms, and microwave power of 100 mW. To ensure no bleed through existed, phase shifts were adjusted to null the conventional spectra at 1 G modulation amplitude and 100 kHz modulation. Each recorded spectrum was the average of three 21 s, 150 G scans.

For each coated cell the pressure was raised in 0.5 MPa increments. To ensure that the system had equilibrated after each change in pressure, spectra were recorded until no difference between subsequent spectra could be discerned (because the polymer films were so thin this occurred within the first two recorded spectra).

From the conventional spectra the extrema separation was measured. Extrema separation is the magnetic field separation between the maximum of the low-intensity line peak and the minimum of the high-intensity line peak in the first-derivative signal from the EPR absorption spectrum (Figure 2). Keinath[14] reported the use of extrema separation to determine glass transition temperatures for amorphous polymers using spin probes from the nitroxide family. In the three-line nitroxide signal the separation distance remains long (approximately 65 G) and unchanged while the polymer is glassy. The separation decreases rapidly as the polymer transitions to a more liquidlike (or plastic) behavior, and once the polymer is beyond this transitional region the separation becomes constant near 35 G (Figure 3). They noticed the glass transition temperature occurred when the spectral width was 50 G for a wide variety of polymers. For this study CO_2-induced glass transition pressure will be determined based on this 50 G extrema separation, because 16-doxyl-stearic acid is a member of the nitroxide family and the separation magnitudes were similar to those observed by Keinath.[14]

This extrema separation method worked well even in the semicrystalline polymers, because a large portion of the probe molecules were trapped in amorphous regions of the maximum 40% crystalline polymer film. As the local viscosity drops in the amorphous regions, the resulting EPR signal will be

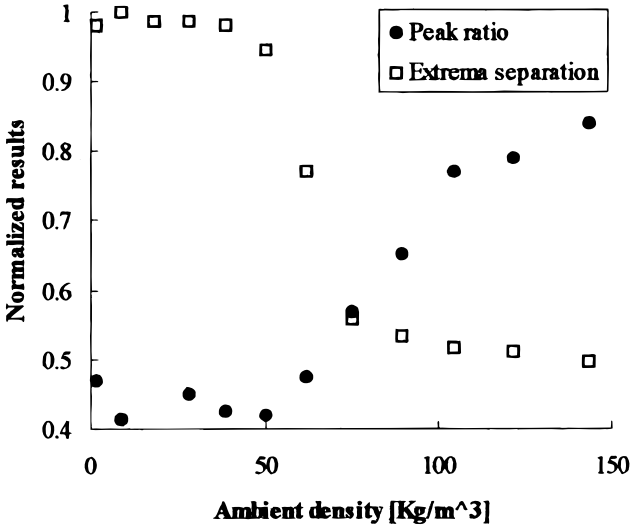

Figure 3. Variation of extrema separation and peak ratio versus carbon dioxide ambient density for 16-doxyl-stearic acid trapped in 65:35 poly(DL-lactide-*co*-glycolide).

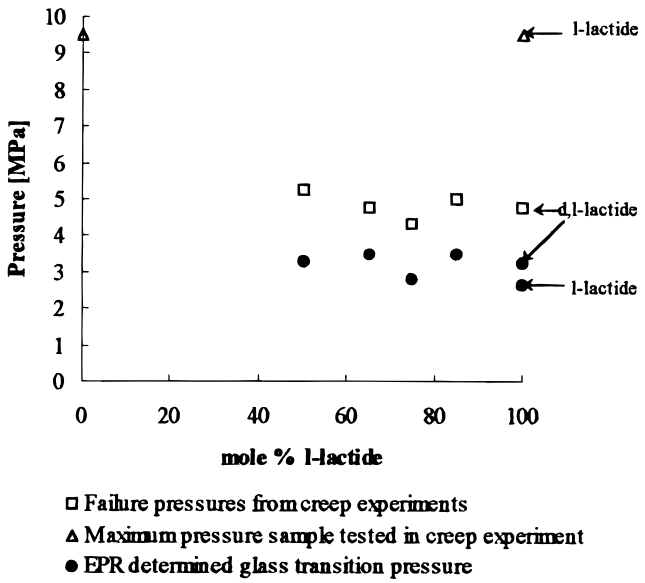

Figure 4. Failure and glass transition pressure comparison for various poly(lactide)−poly(glycolide) copolymers and homopolymers.

significantly stronger than the probe molecules trapped in regions dominated by crystalline structure.

In saturation transfer we desire to select only the portion of the signal that arises from saturation transfer rates. This is done using phase-sensitive detection where the modulation the frequency is 50 kHz while the phase-sensitive detection remains at 100 kHz. For this method the greatest sensitivity was found to be out-of-phase with respect to the second harmonic of the modulation. Once satisfactory spectra are obtained, Thomas et al.[15] showed that following the growth or decay of an intermediate peak with respect to a peak on a turning point was a good indication of how the local viscosity around the probe molecule changes. They determined that this ratio was linearly proportional to the ratio of sample temperature to local viscosity (T/η). For a nitroxide probe, during the transition from a glassy polymer to a more plastic behavior the slope of the low-intensity line in the conventional spectra undergoes the most significant change of the three-line signal. Further, the low-intensity line will remain fairly constant upon the completion of the glass transition. Therefore, this study monitors the relative peak height between the low and intermediate negative signals from second harmonic saturation transfer spectra (Figure 2). The ratio will be small and constant in the glassy region and will rapidly change to a near unity and constant value in the fully plastic region (Figure 3). The inflection point from this transition will be considered the glass transition pressure induced by compressed carbon dioxide.

The two techniques result in similar glass transition pressures. From the 65:35 poly(DL-lactide-*co*-glycolide) data presented in Figure 3, we find the glass transition pressure from the extrema separation technique to be 3.0 MPa (CO_2 density = 60 kg/m^3) while the saturation transfer method yields 3.9 MPa (84 kg/m^3). This was the poorest agreement between the two techniques observed in this study. In general, the transition points agreed within approximately ±0.2 MPa (±5 kg/m^3), and the saturation transfer method consistently measured a higher transition value. The glass transition pressures presented in the results are an average of the two methods.

X-ray Diffraction. X-ray diffraction was performed on a Rigaku powder X-ray diffraction instrument at 80 mA and 40 kV. Scans were conducted from 5° to 40° at a step width of 0.05° and a rate of 2 s per step. Polymer powder samples (45 mg) were prepared on a glass slide by gently compressing all the powder onto a strip 12 mm × 25 mm. Although the strip was slightly smaller than the beam width, this method provides a thick layer of polymer that the beam does not penetrate completely. Partial beam penetration of a sample helps make the comparison of signal magnitude from various samples less dependent on sample quantity and more statistically reliable. The spectral contribution resulting from the exposed portion of the glass slide is far from the region of interest and can be assumed negligible.

Dynamic Mechanical Analyzer. Representative crystalline and amorphous Young's moduli were obtained using a Perkin-Elmer dynamic mechanical analyzer (DMA model 7e). The analyzer was run in the three-point bend mode with a static load of 50 mN and a dynamic load of 10 mN. Amplitude control was set to 8 μm displacement and tension control to 120%. The forcing amplitude was monitored over the entire operating conditions and found to remain nearly constant. The forcing frequency was 1 Hz. Rectangular amorphous polymer samples were approximately 3 mm wide, 1.3 mm thick, and 12−15 mm long. The support holder had pressure points 10 mm apart. Sample moduli were observed from thermal scans from temperatures well below the glass transition (0 °C) to a temperature 20 deg above the glass transition (80 °C) at a heating rate of 3 °C/min. The representative crystalline modulus was determined from the measurements far below the glass transition temperature where temperature dependence is minor. The amorphous modulus was determined from the measurements far above the glass transition where once again temperature dependence has become minor.

Differential Scanning Calorimeter. X-ray diffraction crystallinities were verified using a Perkin-Elmer differential scanning calorimeter (DSC model 7) with a Nesslab RTE-111 chiller set to 0 °C and a nitrogen purge. Thermal scans of 2 mg powder samples were conducted twice. The first scan heated the sample at 10 °C/min to 160 °C and cooled back to room temperature at 30 °C/min. This step improves the polymer contact with the pan and relaxes any material strains that may exist. In the second scan the samples were heated at 10 °C/min from 25 to 220 °C. Crystallinity was determined from subtracting the enthalpy of recrystallized (area under the normalized recrystallization exotherm) from the enthalpy of fusion (area under the normalized melting endotherm) divided by the enthalpy of a 100% sample (93.6 J/g[16]).

Results and Discussion

EPR and mechanical creep experiments were conducted on polymer samples ranging from pure poly(glycolide) to pure poly(lactide) and several of their copolymers. The range of copolymer composition for the amorphous results is required to decipher whether deviations in EPR and creep data result from crystal-

Table 1. Young's Moduli for Various Polymers Studied

polymer	Young's modulus [MPa]	reference
poly(L-lactide)	~4000	Amecke et al.[17]
poly(DL-lactide)	~3000	Amecke et al.[17]

linity or chemical composition. Figure 4 shows the transition pressures at 35 °C for both the creep and EPR experiments. Failure pressures for the poly(L-lactide) and poly(glycolide) specimens were not obtained because of the pressure limitations of the current apparatus. Instead, specimens showed no measurable change in length or surface texture after 4 h at 9.5 MPa.

The glass transition pressures determined using EPR are relatively invariant with copolymer composition, indicating the CO_2 interaction characteristics are similar with increasing glycolide composition. The same trend occurs for failure pressures of the amorphous polymers. However, the measured failure pressures always remained slightly higher than the glass transition pressure for the amorphous copolymers and poly(DL-lactide) samples. This nearly uniform discrepancy is most likely caused by the difference in excitation frequency in the measurement technique. Kumler and Boyer[18] show for various polymers that if one takes into account the change in excitation frequency (EPR = 100−50 kHz, creep ≪ 1 Hz) the transitions will agree. A similar adjustment in the magnitude of the EPR glass transition pressure is expected for the semicrystalline homopolymers because of similar chemical composition. Regardless, the mechanical creep data indicate that the semicrystalline poly(L-lactide) and poly(glycolide) homopolymers maintain sample shape far above the glass transition pressure determined from EPR spectrometry.

To understand the disagreement between the EPR and creep pressure transitions, we must first understand what physical property the creep experiment measures. Typical creep experiments measure the change in sample length with time ($\Delta l/l_0 t = \epsilon/t$). The current creep experiment measured or observed the change in creep rate due to solvent uptake. At small elongations, the stress (σ) experienced by the samples is constant. Therefore, any change in elongation rate must result from a decrease in Young's modulus ($E = \sigma/\epsilon$). Hence, the creep experiment discussed in this paper effectively measures the change in Young's modulus with CO_2 uptake.

In the absence of compressed CO_2 the Young's moduli of the various polymers studied are on the same order of magnitude (Table 1), and all exhibit similar glass transition pressures. But our experiments suggest that the semicrystalline and amorphous polymer moduli diverge above the glass transition pressure. Janzen[19] suggests that the behavior of Young's modulus above the T_g yet below the melt temperature of a semicrystalline polymer can be computed based on the embedding (or "self-consistent field") approach. This predictive approach assumes no slip occurs at the interface between phases (amorphous phase, a, and crystalline phase, c). Further the model assumes a simple spherical geometry for the dispersed phase in order to solve for material properties based on the volume fraction (ϕ) and the properties of the two phases present.[19,20]

The model consists of four equations (below) and eight independent vairables (K, K_a, K_c, G, G_a, G_c, ν, E). ν can be found in the literature,[21] and G_a and G_c are determined using amorphous and crystalline values of Young's modulus, E, respectively. A solution is obtained for each crystallinity volume fraction iteratively by initially guessing that the shear modulus, G, is equal to the amorphous value.

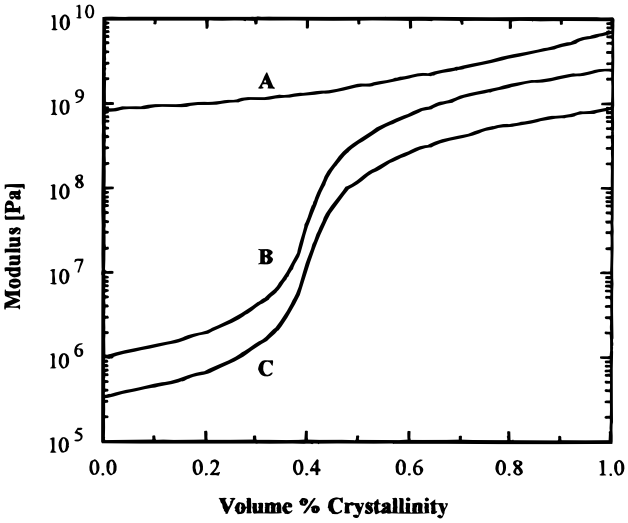

Figure 5. Self-consistent prediction of mechanical property variation with crystalline volume fraction for poly(lactide): (A) bulk modulus, (B) Young's modulus, and (C) shear modulus.

$$K = \frac{K_a K_c + A_k(\phi_a K_a + \phi_c K_c)}{A_k + \phi_c K_a + \phi_a K_c} \quad \text{(bulk modulus)}$$

$$G = \frac{G_a G_c + A_g(\phi_a G_a + \phi_c G_c)}{A_g + \phi_c G_a + \phi_a G_c} \quad \text{(shear modulus)}$$

$$A_g = \frac{G(9K + 8G)}{6(K + 2G)}$$

$$\nu = \frac{3K + 2G}{2(G + 3K)} \quad \text{(Poisson's ratio)}$$

$$E = 2(1 + \nu)G \quad \text{(Young's modulus)}$$

Figure 5 shows the predicted variation of mechanical properties in a semicrystalline polymer. The amorphous and crystalline Young's modulus values used in the solution of the model were obtained from dynamic mechanical analyzer experiments conducted on poly(lactide) samples in our laboratory. The 3 orders of magnitude increase in Young's and shear modulus is typical for semicrystalline polymers. Near 30% crystallinity by volume, the Young's modulus becomes twice that of the purely amorphous polymer and 20 times larger by 40% crystallinity. Slow cooling used in the formation of the polymer tensile specimen leads to near maximum crystallinity. Gilding and Reed[22] published maximum crystallinity levels for lactide−glycolide copolymers. The homopolymers poly(glycolide) and poly(L-lactide) are semicrystalline with crystallinity levels larger than 30%, while the poly(DL-lactide) is amorphous. Copolymers containing DL-lactide and glycolide remain amorphous until over 70% of the copolymer chain consist of glycolide blocks. As a result, we only expect the semicrystalline poly(L-lactide) and poly(glycolide) homopolymers to retain Young modulus values 20 times larger than the amorphous polymer in the presence of high-pressure CO_2. Larger Young's moduli or substantially lower creep rates in the semi-

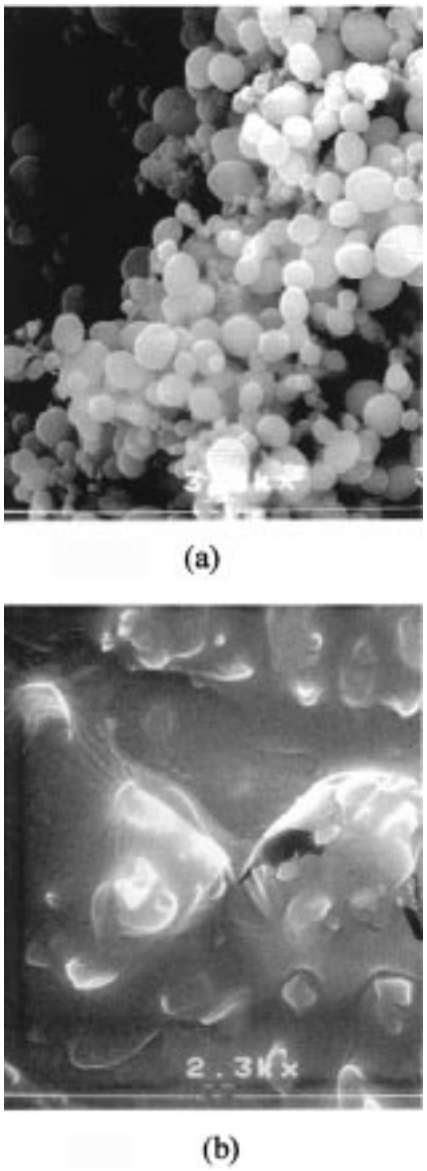

Figure 6. SEM photomicrographs of (a) poly(L-lactide) and (b) 50:50 poly(DL-lactide-*co*-glycolide).

crystalline homopolymers are consistent with our inability to reach a failure pressure with these samples.

Attempts were made to process each of the various polymer samples using the PCA technique.[1] Each polymer is dissolved in CH_2Cl_2 (10 mg/mL) and injected into a compressed carbon dioxide environment using an ultrasonic nozzle. At 35 °C and 8.5 MPa CH_2Cl_2 becomes highly soluble in CO_2, resulting in the rapid extraction of CH_2Cl_2 and precipitation of polymer microparticles. When operated in a continuous flow fashion (1 mL/min polymer solution; 25 mL/min liquid CO_2), the micron-sized particles are collected on a 0.2 μm filter downstream of the precipitation region.

Figure 6a shows a SEM photomicrograph of the semicrystalline poly(L-lactide) particles formed by PCA. The light regions are the polymer particles, which are on the order of 1−2 μm in diameter. Tests using the same operating conditions, but dissolving poly(glycolide) in hexafluoro-2-propanol (Strem Chemicals) yielded particle morphologies very similar to those seen in the poly(L-lactide) photomicrograph except for a slight decrease in particle diameter. Tests conducted on the amorphous poly(DL-lactide) and poly(DL-lactide-*co*-glycolide) yielded particle morphologies substantially different than those observed in the semicrystalline polymers. Figure 6b shows a SEM photomicrograph of 50:50 poly(DL-lactide-*co*-glycolide) after PCA processing. The morphology presented in this photomicrograph is representative of the behavior exhibited by all of the amorphous polymers. The light region is continuous, indicating a thin film connecting regions of denser polymer resulting from severely agglomerated polymer particles.

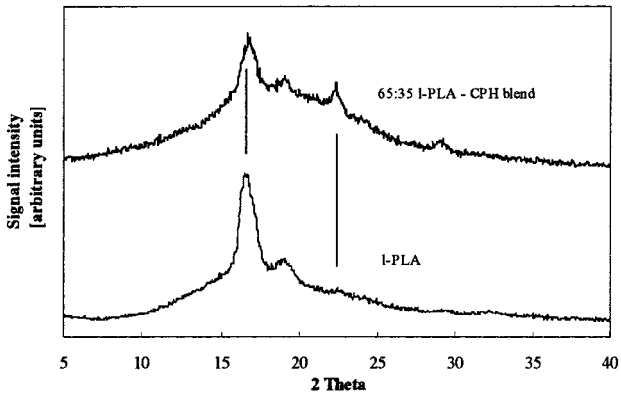

Figure 7. X-ray powder diffraction scans of polymer microparticle formed by PCA: (a) poly(L-lactide) and (b) 60:30 blend of poly(L-lactide) and CPH.

X-ray diffraction and DSC crystallinity measurements of the poly(L-lactide) particles after processing show crystallinity levels near 25%. According to the embedding approach (Figure 5) a crystallinity of 25% should not raise the Young's modulus substantially, but long polymer chains lead to entanglement between the amorphous and crystalline phase. The effects of phase entanglement are not captured in the spherical assumption of the theoretical model described. As entanglement increases, a smaller dispersed phase volume is required to affect bulk properties. As a result, a large change in Young's modulus at 25% crystallinity may not be a poor expectation from 100 000 molecular weight poly(L-lactide) molecules. Past literature indicates that the crystalline structure in a polymer system, such as poly(vinyl chloride), can begin to control a material's mechanical strength at crystallinities as low as 3%.[23,24] In addition, the X-ray diffraction and DSC measurements make no distinction between surface layer and bulk crystallinity. If the majority of the crystalline domains are located at the surface of the particle, the local crystallinity maybe quite large, resulting in a strong exterior shell.

Several attempts were made to determine a critical crystallinity for poly(L-lactide), below which particle shape could not be maintained during PCA processing. We lowered crystallinity levels in the particles through the addition of impurities. The addition of CO_2-insoluble molecules with a molecular structure different than L-lactide in the CH_2Cl_2−polymer solution may limit the crystalline levels obtained during PCA. Further, varying the volume fraction of impurity should allow manipulation of the resulting processed particle crystallinity. Impurities such as semicrystalline linear 1,6-bis(carboxyphenoxy)hexane (CPH) seemed to have little effect on the particle morphology. An X-ray diffraction scan (Figure 7) revealed that the resulting particles have partially phase separated into different crystalline regions which help maintain the polymer's mechanical strength. The first peak in Figure 7 represents crystal-

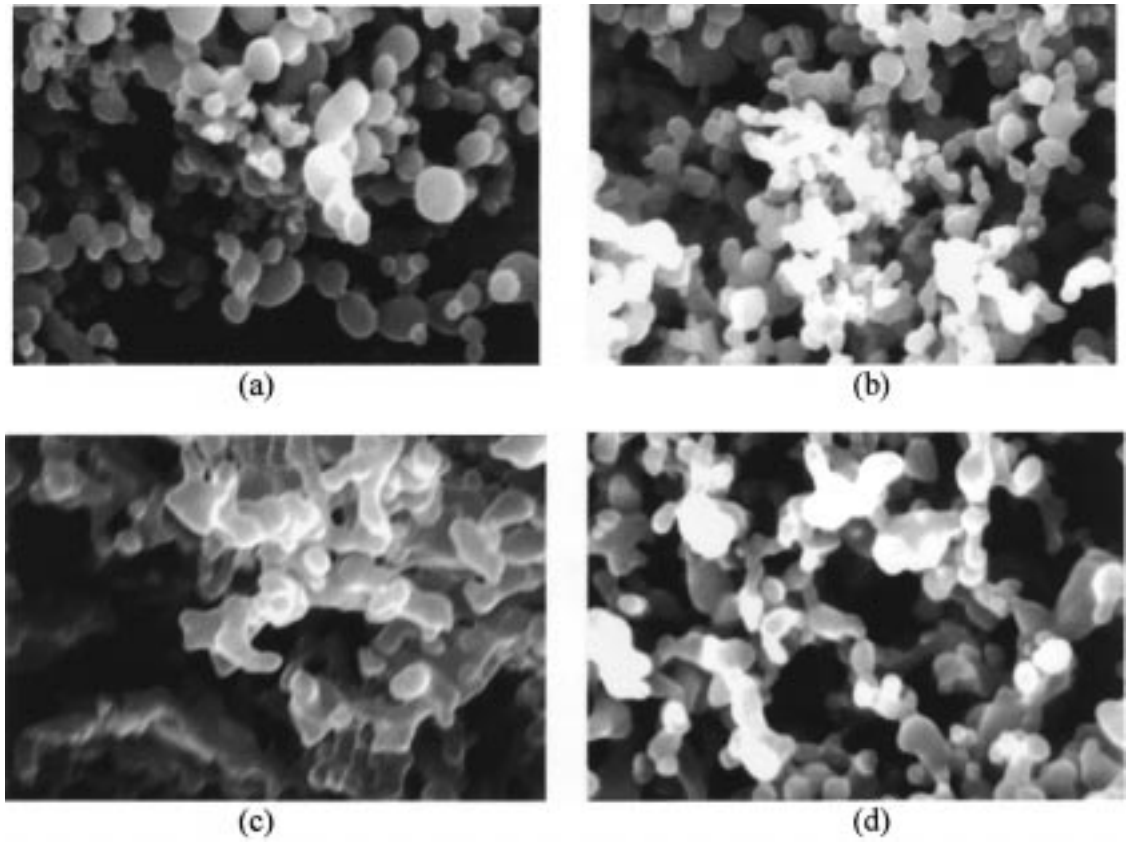

Figure 8. SEM photomicrographs of polymer microparticles formed using precipitation with a compressed antisolvent at 8.5 MPa, 35 °C, solvent flow rate = 1 mL/min, CO_2 flow rate = 25 mL/min, and an original polymer to solution loading of 10 mg/mL: (a) 100% poly(L-lactide), 26% crystalline; (b) 80% poly(L-lactide)−20% poly(DL-lactide) blend by mass, 19% crystalline; (c) 60% poly(L-lactide)−40% poly(DL-lactide) blend by mass, 12% cystalline; (d) 85:15 poly(L-lactide-*co*-glycolide), 15% crystalline.

lized poly(L-lactide), whereas the second dominate peak represents crystallized CPH.

Success in lowering the particle crystallinity was obtained through the addition of amorphous poly(DL-lactide). Figure 8 shows the resulting SEM micrographs from PCA processed poly(L-lactide) particles with 0, 20, and 40% by mass poly(DL-lactide) (26, 19, and 12% crystallinity, respectively). As particle crystallinity decreases, agglomeration becomes more prevalent, dominating morphology near 12% crystallinity. To verify this trend was not a result of impurities phases separating and depositing on the particle surface, we processed 85:15 poly(L-lactide-*co*-glycolide), a block copolymer with a maximum crystallinity between 15 and 20%.[22] In Figure 8 the poly(L-lactide-*co*-glycolide), 15% crystalline, particles are partially agglomerated. The extent of particle agglomeration exhibited by the poly(L-lactide-*co*-glycolide) particles agrees with the trend established using particles formed through the addition of impurities, displaying a morphology between the 12 and 19% crystalline particles.

We feel that the critical crystallinity required for poly(lactide) or poly(glycolide) to maintain particle morphology during PCA conditions above their glass transition is near 12%. In the PCA process, crystallinity evolves with time as organic solvent is removed from the polymer. The final crystallinity measured in this paper may not be the actual particle crystallinity at the time of impact with adjacent particles. As a result, the actual critical crystallinity to maintain particle morphology may be less than 12%. In addition, this critical crystallinity value will vary from polymer to polymer.

Conclusion

Absorption of compressed CO_2 into a polymer can suppress the glass transition temperature below the operating temperature of a PCA system. This T_g suppression results from interaction characteristics between the pure polymers and the CO_2 diluent (Condo et al., 1992; Kalospiros and Paulaitis, 1994). However, polymers can retain particle morphology above their T_g because of moderate crystalline volume fractions that slow the relaxation of mechanical strength, causing a creep rate low enough to limit agglomeration. As a result, semicrystalline polymers can be expected to retain microparticle morphology during PCA conditions above their glass.

References and Notes

(1) Falk, R.; Randolph, T. W.; Meyer, J. D.; Kelly, R. M.; Manning, M. C. *J. Controlled Release* **1997**, *44*, 77−85.
(2) Falk, R.; Randolph, T. W. *Pharm. Res.* **1998**, *15* (8), 1233−1237.
(3) Randolph, T. W.; Randolph, A. D.; Mebes, M.; Yeung, S. *Biotechnol. Prog.* **1993**, *9*, 429−435.
(4) Dixon, D. J.; Johnston, K. P.; Bodmeier, R. A. *AIChE J.* **1993**, *39* (1), 127−139.
(5) Hojo, H.; Findley, W. N. *Polym. Eng. Sci.* **1973**, *13*, 255−265.
(6) Wissinger, R. G.; Paulaitis, M. E. *Ind. Eng. Chem. Res.* **1991**, *30*, 842−851.
(7) Wang, W. V.; Kramer, E. J.; Sachse, W. H. *J. Polym. Sci., Part B: Polym. Phys.* **1982**, *20* (6), 1371−84.
(8) Chiou, J. S.; Barlow, J. W.; Paul, D. R. *J. Appl. Polym. Sci.* **1985**, *30*, 2633−2642.
(9) Condo, P. D.; Johnston, K. P. *J. Polym. Sci., Part B: Polym. Phys.* **1994**, *32*, 523−533.

(10) Condo, P. D.; Sanchez, I. C.; Panayiotou, C. G.; Johnston, K. P. *Macromolecules* **1992**, *25*, 6119−6127
(11) Kalosiros, N. K.; Paulaitis, M. E. *Chem. Eng. Sci.* **1994**, *49* (5), 659−668.
(12) Bodmeier, R.; Wang, H.; Dixon, D. J.; Mawson, S.; Johnston, K. P. *Pharm. Res.* **1995**, *12* (8), 1211−1217.
(13) Berens, A. R.; Huvard, G. S. *Supercritical Fluid Science and Technology*, ACS Symposium Series 406; Johnston, K. P., Penninger, J. M. L., Eds.; American Chemical Society: Washington, DC, 1989; pp 204−223.
(14) Keinath, S. E. *International 17th Symposium on Order in the Amorphous "State of Polymers"*; 1985; pp 187−219.
(15) Thomas, D. D.; Dalton, L. R.; Hyde, J. S. *J. Chem. Phys.* **1976**, *65* (8), 3006−3024.
(16) Agarwal, M.; Koelling, K. W.; Chalmers, J. J. *Biotechnol. Prog.* **1998**, *14*, 517−526.
(17) Amecke, B.; Bendix, D.; Entenmann, G. *Clin. Mater.* **1992**, 47−50.
(18) Kumler, P. L.; Boyer, R. F. *Macromolecules* **1976**, *9*, 903−910.
(19) Janzen, J. *Polym. Eng. Sci.* **1992**, *32* (17), 1242−1254.
(20) McGee, S.; McCullough, R. L. *Polym. Compos.* **1981**, *2* (4), 149−161.
(21) Brandrup, J.; Immergut, E. H. *Polymer Handbook*, 3rd ed.; John Wiley & Sons: New York, 1989.
(22) Gilding, D. K.; Reed, A. M. *Polymer* **1979**, *20*, 1459−1464.
(23) Walter, A. T. *J. Polym. Sci.* **1954**, *13*, 207.
(24) Koleske, J. V.; Wartman, L. H. *Poly(vinyl chloride)*; Gordon and Breach Science Publishers: New York, 1969; pp 67−69.

MA9813035